

TECHNICAL MATERIAL

Estimation of Effective Energy in Phantom in X-ray CT Using Monte Carlo Simulation

Shimpei KONDO^{1*}, Shuji KOYAMA¹

¹Department of Radiological Technology, Graduate School of Medicine, Nagoya University
1-1-20 Daiko-Minami, Higashi-ku, Nagoya, Japan

The aim of research was to estimate X-ray energy spectrum and effective energy in phantom undergoing X-ray CT scan using Electron Gamma Shower 5 Monte Carlo simulation. Radiation source of X-ray CT (TCT-300; Toshiba Medical, Tochigi, Japan) was revolved 360 degrees at intervals of 1 degree around a phantom which was a water cylinder of 32cm diameter. An X-ray CT is generally equipped with the beam-shaping filter in front of the X-ray tube radiation window. For making X-ray CT simulation more concrete, effective energy and dose distribution in each degree of the fan beam after penetrating through the beam-shaping filter were measured with an ionization chamber, which were incorporated in the simulation. The number of photons was counted by the energy for obtaining in-phantom X-ray spectrum in small discs in a cylindrical water phantom, and effective energy was calculated from in-phantom X-ray spectrum. Effective energy is nearly uniformity in the phantom, and an insignificant difference exists between incident and in-phantom X-ray spectrum.

KEYWORDS: X-ray CT, effective energy, beam-shaping filter, Monte Carlo Simulation, EGS5

I. Introduction

X-ray entering into a phantom is absorbed and scattered. In-phantom X-ray spectrum has a potential to differ from incident X-ray spectrum. Nagoya University has small semiconductor dosimeters which are very useful to measure doses in phantom. The X-ray dosimeters have large energy dependence¹⁾ and, are influenced by beam quality changing through phantom substance by X-ray absorption and scattering. Calibration factor for the dosimeters is required to estimate correct absorbed dose. Absorbed dose measured with these dosimeters in the phantom would be able to calibrate using calibration factor for the energy of incident X-ray beam to the phantom. The absorbed dose has, however, some inaccuracy because effective energy (E_{eff}) of in-phantom X-rays is different from that of incident X-rays. Effective energy of a certain X-ray beam is defined as the energy of mono-energetic X-ray beam that has the same half-value layer. It is important to measure X-ray energy spectrum and effective energy in phantom to know appropriate calibration factor. To measure the energy spectrum in the phantom with spectrometer or half-value layer in the phantom with ionization chamber, semiconductor dosimeter, etc, this is the best way of getting calibration factor. However, it is impossible to measure those values in experimental geometry. Monte Carlo simulation has the advantage of being able to calculate difficult measurement situation. In this study, in-phantom X-ray energy spectrum and effective energy were estimated by using Monte Carlo simulation.

II. Material and Methods

X-ray energy spectrum and effective energy in a phantom undergoing X-ray CT scan were estimated by Electron Gamma Shower 5 (EGS5) Monte Carlo simulation code.

1. Simulation Geometry

Figure 1 shows geometry of this calculation. X-ray-focus to isocenter distance was 60 cm. X-ray CT has a fan beam, and the form of incident fan beam was incorporated in the simulation. The X-ray tube was revolved 360 degrees at intervals of 1 degree around the phantom. The fan beam angle was 36 degrees and the beam thickness was 0.5 cm.

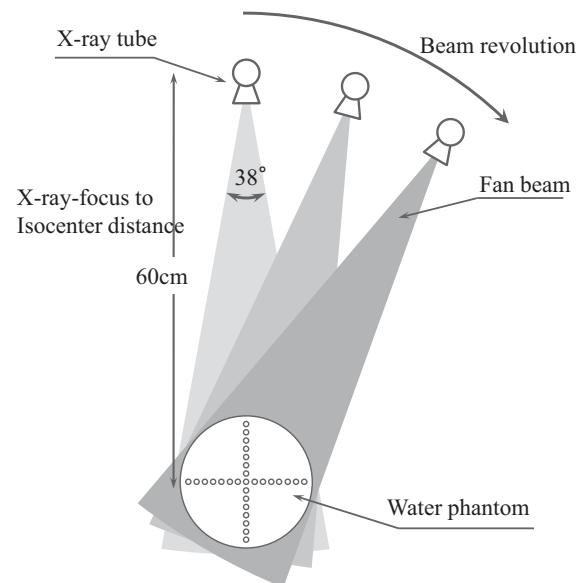


Fig. 1 Geometry of calculation code undergoing X-ray CT.

*Corresponding Author, E-mail:kondo.shimpei@e.mbox.nagoya-u.ac.jp
© 2012 Atomic Energy Society of Japan, All Rights Reserved.

Figure 2 shows geometry of the cylindrical water phantom. The cylindrical phantom consisted of water, 32 cm in diameter and 20 cm in length. Twenty nine small water discs of 1 cm diameter were put inside the phantom along horizontal and vertical axis of an axial plane. The outmost discs in each line were placed at 0.7, 1.0, 1.3, 1.6 cm from the phantom surface, and center-to-center distance of each disc was 1.2 cm.

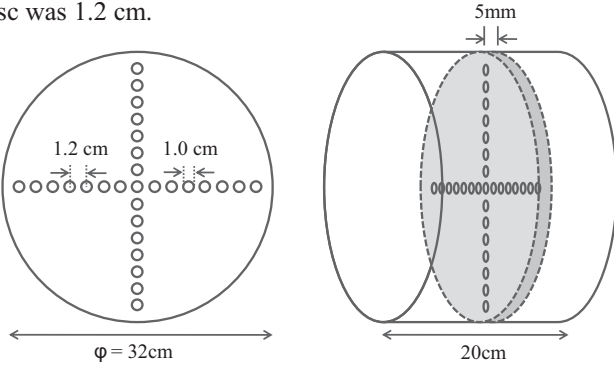


Fig. 2 Geometry of water phantom.

2. Beam-shaping filter incorporated in simulation

X-ray CT is generally equipped with a beam-shaping filter in front of the X-ray tube radiation window. Beam-shaping filter (usually referred to as a “bow-tie” filter) is used to shape the beam and to ensure more constant signal to all detectors, so that there are more and softer X-rays in the central portion of the fan beam and fewer and harder X-rays on the periphery. **Figure 3** indicates basic concept of beam-shaping filter and fan beam.

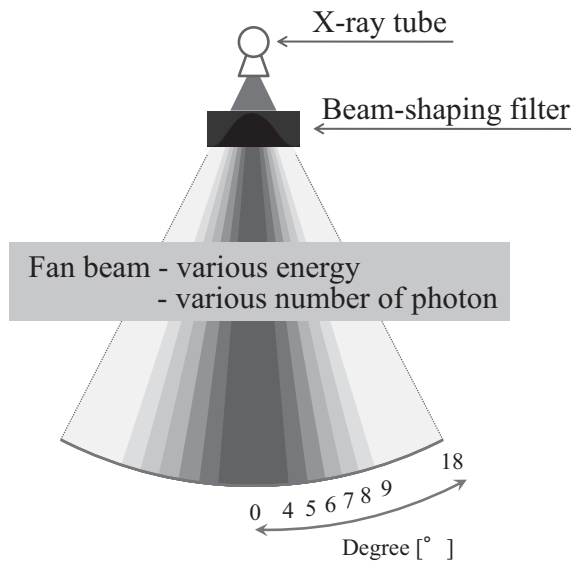


Fig. 3 Fan beam of X-ray CT after penetrating through beam-shaping filter.

For making X-ray CT simulation more concrete, the effect of beam-shaping filter contributed to X-ray attenuation and beam hardening, must be incorporated in incident fan beam in the simulation. Detailed information of the beam-shaping filter is normally closed by the manufacturer. Effective energy and dose distribution in each degree of the fan beam after penetrating through the beam-shaping filter were measured with an ionization chamber in an X-ray CT

(TCT-300; Toshiba Medical, Tochigi, Japan)(**Figure 4**), which were incorporated in the simulation. At an X-ray tube of 120kVp, seven different X-ray spectrums, E_{eff} was 54, 57, 59, 62, 64, 72, and 73 keV from the center part to the outer part, were used in the each part of incident fan beam (0-4, 4-5, 5-6, 6-7, 7-8, 8-9, and 9-18 degrees)². The number of photon corresponding to dose distribution data was used in each degrees of incident fan beam.

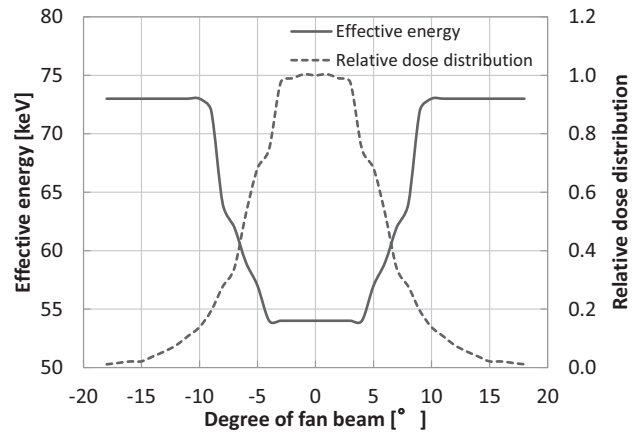


Fig. 4 Effective energy and dose distribution data.

3. Obtaining in-phantom spectrum and effective energy

The photon passing through the small disc inside the phantom was counted by photon energy, and those were used for calculating in-phantom energy spectrum and effective energy along horizontal axis and vertical axis of an axial plane of the phantom. The total number of photon source was 1.44×10^9 . Statistical error was determined less than 1.0 % in the simulation.

III. Results

Change of effective energy in the phantom is shown in **Figure 5**. Effective energy is nearly uniformity in the phantom, and the spread between the highest and lowest in-phantom effective energy ($E_{eff-high}$, $E_{eff-low}$) was less than 1.0 keV. Fluctuation of effective energy curve was read graphically with statistical error of less than 1.0 % in the simulation.

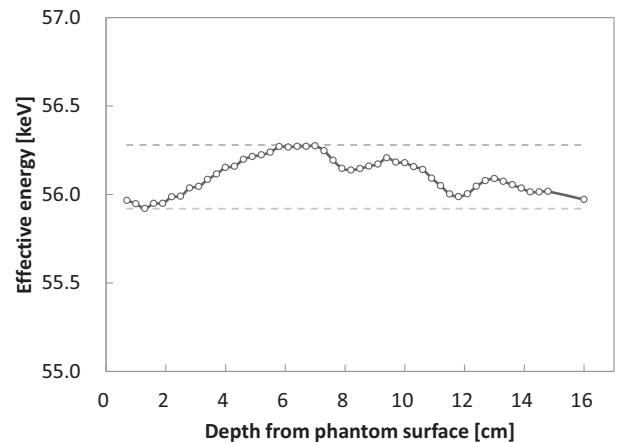


Fig. 5 Change of in-phantom effective energy in each depth from the phantom surface.

A comparing in-phantom X-ray spectrum with $E_{\text{eff-high}}$, $E_{\text{eff-low}}$, and incident X-ray spectrum is shown in **Figure 6**. The beam quality of both in-phantom X-ray spectrum with $E_{\text{eff-high}}$ and $E_{\text{eff-low}}$ was slightly harder compared to that of incident X-ray spectrum.

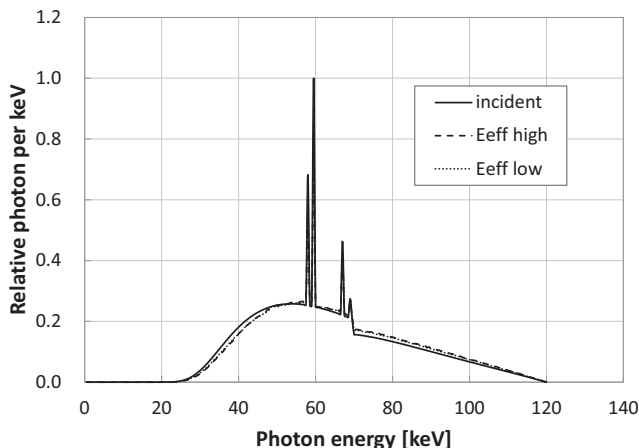


Fig. 6 Comparison between incident X-ray spectrum and in-phantom X-ray spectrum with $E_{\text{eff-high}}$ or incident X-ray spectrum and in-phantom X-ray spectrum with $E_{\text{eff-low}}$.

IV. Discussion

One would think that X-ray entered in phantom is absorbed, and beam quality becomes harder. In this research, an insignificant difference existed between incident and in-phantom effective energy. Furthermore effective energy was nearly uniformity in the phantom. At the point of each depth, low energy component of the X-ray spectrum was reduced by beam hardening. In contrast, low energy X-rays generated in another area by Compton scattering was contributed to the spectrum. X-ray spectrum in phantom has possibilities not only being harder but also being softer. The proportion between beam hardening and Compton scattering is important component of changing effective energy process. **Figure 7** shows change of in-phantom effective energy for each energy spectrum of seven parts of the fan beam. The graph simply indicated that in-phantom effective energy decreased with increasing depth when incident X-ray effective energy was larger than about 60 keV, increased with increasing depth when incident X-ray effective energy was less than about 60 keV. In the former, Compton scattering had a much greater impact on in-phantom X-ray spectrum than beam hardening, and the latter, opposite effect was observed.

Fluctuation of the effective energy in **Figure 5** was caused by the presence of the boundary of each section assigned different energy spectrum varied with the angle of fan beam. Another simulation using single energy spectrum in the fan beam confirmed that fluctuations were not occurring in the phantom. In a practical situation, there is no boundary in X-ray CT fan beam, therefore, the fluctuation of effective energy in **Figure 5** is not meaningful in the simulation.

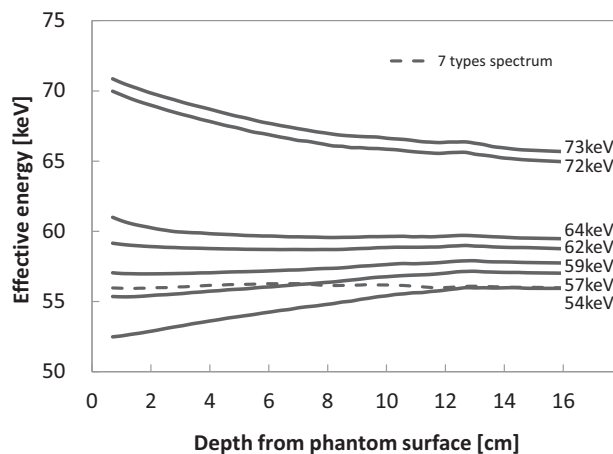


Fig. 7 Changing of in-phantom effective energy in using single type of energy for the fan beam. Each energy value corresponding with solid lines is effective energy of incident X-ray spectrum, the dashed line is similar to the line showed in **Figure 5**.

X-ray CT also has complex factors with change of in-phantom effective energy, which are the effects of beam-shaping filter and revolving fan beam. Projected figure in each revolving angle is shown in **Figure 8**. The isocenter disc is exposed by single energy spectrum, but the other part discs are exposed by various types of incident X-ray spectrum.

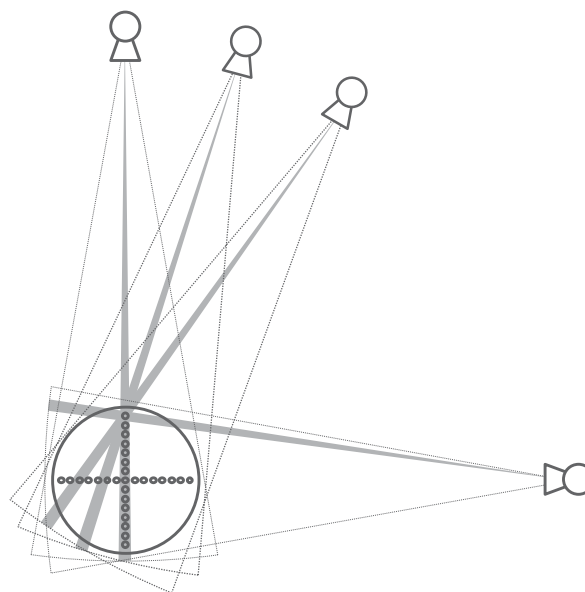


Fig. 8 Photon counting part was projected in each rotating angle.

Figure 9 shows the energy dependence of small semiconductor dosimeter owned by Nagoya University. The difference of sensitivity of small semiconductor between incident and in-phantom effective energy is shown in **Table 1**. Relatively small changing of effective energy in phantom had an insignificant effect on calibration factor for the semi-conductor dosimeters.

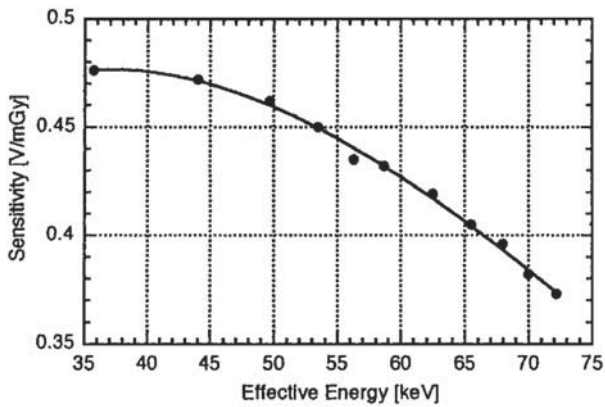


Fig. 9 Energy dependence of small semiconductor dosimeter (made by T Aoyama; Nagoya University 2002)¹⁾.

Table 1 Difference of sensitivity of small semiconductor dosimeter for effective energy.

	Effective energy	Sensitivity	Difference for incident X-ray	
	[keV]	[V/mGy]	[V/mGy]	[%]
incident X-ray	54.00	0.448	-	-
in-phantom X-ray	56.28 (high)	0.440	-0.008	-1.79
	55.92 (low)	0.442	-0.006	-1.34

V. Conclusion

In-phantom X-ray spectrum and effective energy undergoing X-ray CT are estimated by using Monte Carlo simulation (EGS5). Effective energy is nearly uniformity in each depth of the phantom, and an insignificant difference exists between in-phantom and incident X-ray spectrum.

Recently, small semiconductor x-ray dosimeter installed in critical organ sites in an anthropomorphic phantom is used to estimate tissue or organ doses and the effective doses to patient exposure from diagnostic X-ray¹⁾. Using Monte Carlo simulation (EGS5) to estimate in-phantom effective energy gives results that relatively small changing of effective energy has an insignificant effect on calibration factor for energy dependence. The calibration factor for energy dependence of in-phantom semiconductor dosimeter is able to determine by the easily obtainable effective energy of incident X-ray.

References

- 1) T. Aoyama, S. Koyama, C. Kawaura, An in-phantom dosimetry system using pin silicon photodiode radiation sensors for measuring organ doses in X-ray CT and other diagnostic radiology, *Medical Physics* 29 (7) (2002) 1504-1510.
- 2) M. Tucker, G. Barnes, D. Chakraborty, Semiempirical model for generating tungsten target X-ray spectra, *Medical Physics* 18 (2) (1991) 211-218.